A method to predict the uncompleted climate transition process

Pengcheng Yan[1, 3], Guolin Feng[2], Wei Hou[2]

[1]{Institute of Arid Meteorology, China Meteorological Administration, Key Laboratory of Arid Climatic Change and Reducing Disaster of Gansu Province, Key Laboratory of Arid Climatic Change and Reducing Disaster of China Meteorological Administration, China}

[2]{National Climate Center, China Meteorological Administration, China}

[3]{China Meteorological Administration Training Center, Beijing, China}

[*]Correspondence to: Wei Hou (houwei@cma.gov.cn)

Abstract

Climate change is expressed as a climate system transiting from the initial state to a new state in a short time. The period between the initial state and the new state is defined as transition process, which is the key part to connect the two states. By using a piece-wise function, the transition process is stated approximately (Mudelsee, 2000). However, the dynamic processes are not included in the piece-wise function. Thus, we had proposed a method (Yan et al, 2015, 2016) to study the transition process by using a continuous function. In this manuscript, this method is developed to predict the uncompleted transition process based on the dynamic characteristics of the continuous function. We introduce this prediction method in details and apply it to three ideal time sequences and the Pacific Decadal Oscillation (PDO). The PDO is a long-lived El Niño-like pattern of Pacific climate variability (Barnett et al, 1999). This method reveals a new quantitative relationship during the transition process, which explores a nonlinear relationship between the linear trend and the amplitude (difference) between the initial state and the end state. As the transition process begins, the initial state and the linear trend are estimated. Then, according to the relationship, the end state and end moment of the uncompleted transition process is predicted.

Keywords

Prediction method; Transition process of abrupt change; System stability; Pacific

Decadal Oscillation

1. Introduction

A system transiting from one stable state to another in a short period is called abrupt change (Charney and DeVore, 1979; Lorenz, 1963, 1979). The abrupt change system has two or more states (Goldblatt et al, 2006; Alexander et al, 2012), the system swings between these states that are also called attractors in physics. This phenomena is verified in many fields including biology (Nozaki, 2001), ecology (Osterkamp et al, 2001), climatology (Thom, 1972; Overpeck and Cole, 2006; Yang et al, 2013a, 2013b), brain science (Sherman et al, 1981), etc. The latest observed climate change event is global warning hiatus, which has been studied deeply by many researchers (Amaya et al, 2018; Kosaka and Xie, 2013; Yang et al, 2017). Seven different kinds of abrupt changes are mentioned in Thom's research(1972). Over the last several decades, many methods have been proposed to identify different kinds of abrupt change (Li et al, 1996), such as Moving T-Test, Cramer's (Wei, 1999), Mann-Kendall (MK, Goossens and Berger, 1986), Fisher (Cabezas and Fath, 2002), etc. It is noticed that most abrupt change detection methods suggest that the abrupt change is around a turning point. The significant difference between the average values of the two sequences on both two sides of the turning point is defined as the index to measure the abrupt change. This kind of detection method has a drawback. It is difficult to detect the abrupt change that occurs at the end of sequence.

Mudelsee (2000) studied the abrupt change of a time sequence and illustrated that abrupt change has a duration, which can be quantitatively described with a piece-wise (ramp) function. We developed the detection method by using a continuous function to replace the ramp function(Yan et al, 2014, 2015). The new method can confine the beginning and ending points of abrupt change and quantitatively describes the process of abrupt climate change, and three parameters are introduced. A quantitative relationship among the parameters is revealed (Yan et al, 2015). The relationship could be used to predict the end moment (state) if the system

had left the original state but not yet reached to the new state, which is defined as an uncompleted transition process.

In this manuscript, three ideal time sequences are tested to study the prediction method. The prediction method is also applied to study the climate transition process of the PDO, which is an important signal that reveals climatic variability on the decadal timescale (Mantua et al, 1997; Barnett et al, 1999; Zhang et al, 1997; Yang et al, 2004). Previous studies (Lu et al, 2013; Trenberth and Hurrell, 1994) have indicated that there are many abrupt changes in the PDO over the past 100 years. Most researches mentioned the climate changes happened in the 1940s and 1970s. During the 1940s, the PDO transited from a high state to a low state, while during the 1970s, it did the opposite. All of these changes and their processes had been studied in our previous research (Yan et al, 2015 2016). The climate transition processes were explored clearly. However, we still can not know when the transition processes finish their increasing or decreasing to a stable state if the transition process has begun. We develop a new method to predict the end state and the end moment of a transition process based on the quantitative relationship.

2. Methods

It is necessary to describe the transition process quantitatively before the prediction of the uncompleted climate transition process. We had proposed a detection method by using the logistic model to obtain a transition process. In section 2.1, the method is introduced briefly. On the basis of the detection method, the prediction method for studying the uncompleted transition process is further developed in section 2.2.

2.1 The detection method of transition process

The real time sequence changes abruptly as shown in figure 1a, and the system jumps to a high state in point C. If the period around point C is observed on a shorter time scale (as shown figure 1b), a transition period is obtained, and it is a part of the

original time sequence. In fact, many abrupt changes could be considered to be a transition period with a more detailed view. The transition period was expressed with a ramp function in Mudelsee's research (2000) as shown in figure 1c, and the time sequence is divided into three segments, including two equilibrium states and one increasing state. The ramp function is as follows:

$$x_t = \begin{cases} x_1 & t \le t_1 \\ x_1 + (t - t_1)(x_2 - x_1)/(t_2 - t_1) & t_1 < t \le t_2 \\ x_2 & t > t_2 \end{cases}, \quad (1)$$

where t represents time, and x_t represent the system states, which is obtained by the linear regression method. It is noted that the climate system is continuous; it is even the sampling sequence that makes it is discontinuous. We used a continuous function to express this transition period approximately, and we also created a novel method to detect the transition period (Yan et al, 2015). Here, the detection method is introduced briefly. The continuous evolution of the logistic model is consistent with the transition process (May, 1976), which is shown in figure 1d. The modified logistic model is expressed as follows:

$$\dot{x} = k(x - u)(v - x). \quad (2)$$

Parameters u and v represent the two equilibrium states respectively. Parameter k represents the switching between different states, and it is defined as the instability parameter. As shown in figure 2a, parameters u and v being fixed, and setting k as 0.5, the system transiting to the new state costs a shorter time than that setting k as 0.4. If parameter k is set large enough, the system collapses and becomes chaotic (as shown in figure 2b). When parameter k is set to different values, more situations have been discussed in detail in the previous research (Yan et al, 2016). The result shows that parameter k characterizes the stability of the system (the larger the absolute value, the more unstable the system). According to Thom's theory (1972), the system described by a quartic function would exhibit tipping-point abrupt change in which the system jumps from one state to a new state abruptly. Thus, we did some mathematical derivation to Eq. (2), and the general potential energy is obtained as follows:

$$V_{(x)} = -\int_0^x \ddot{x}dx = -\int_0^x 2k^2\left[x-(u+v)/2\right](x-u)(x-v)dx$$
$$= \frac{k^2}{2}\left[x^4 - 2(u+v)x^3 + \left(u^2+v^2+4uv\right)x^2 - 2(u+v)uvx\right] \quad (3)$$

It means that Eq. (2) describes a system with tipping-point abrupt change. In figure 2c, the potential energy of Eq. (3) is verified to have two states with the lowest energy, and both of them are stable. This bistable structure is common in the climate system (Goldblatt et al, 2006). Therefore, Eq. (2) can be used to describe the abrupt change system, and the parameters represent different key factors of the transition period during abrupt change. Then, the parameters *u, v* and *h* are obtained by the regression method (Huang, 1990; Yang et al, 2013a) by using Eq. (4), where *i*, x_i denote the time and the state of the system at this time, and $\bar{i}, \bar{x}_i$ are their averages respectively. Variable n_2 is the length of the second segment.

$$\begin{cases} v = \sum_{i=1}^{n_1} x_i / n_1 \\ u = \sum_{i=n_1+n_2+1}^{n} x_i / n_3 \\ h = \sum_{i=n_1+1}^{n_1+n_2} \bar{i} \cdot \bar{x}_i \Big/ \sum_{i=n_1+1}^{n_1+n_2} \bar{i}^2 \cdot \end{cases} \quad (4)$$

The linear trend *h* represents the ratio of system state change to time, and it can be expressed by two points on the curve approximately as Eq. (5), where the two points are *A* (x_a, t_a) and *B* (x_b, t_b).

$$h = \frac{x_a - x_b}{t_a - t_b} \quad (5)$$

As shown in figure 2d, the transition period during point *A* (x_a, t_a) and point *B* (x_b, t_b) is approximately linear. Then, we can use the location parameters α, β to express system states x_a and x_b. By solving Eq. (2), the relationship between *x* and *t* is determined.

$$t = \frac{1}{k(u-v)} \ln\left(\frac{x_0-u}{x_0-v} \cdot \frac{x-v}{x-u}\right) + t_0 \quad (6)$$

Then, parameter h is rewritten as Eq. (7). It is noted that the rightmost part is only related to the location parameters α and β, then let it be χ. Then, the relationship of Eq. (7) is rewritten as Eq. (8):

$$h = \frac{x_b - x_a}{\frac{1}{(\mu-\nu)k}\ln\frac{x_0-\mu}{x_0-\nu}\left(\frac{x_b-\nu}{x_b-u}-\frac{x_a-\nu}{x_a-u}\right)} = k(\mu-\nu)^2\frac{(\beta-\alpha)}{\ln\frac{\beta(\alpha-1)}{\alpha(\beta-1)}}, \tag{7}$$

$$h = k\omega^2\chi . \tag{8}$$

In order to determine the value of parameter χ, the relationship among χ, α, β is displayed in figure 3b. The dash line in figure 3a is the profile of the diagonal in figure 3b, which represents that the sum of α and β is 1. Parameter χ changes little when the location parameter varies in a certain range as marked with warm color in figure 3b. It means that the closer the points (A and B) are to the middle point, the more significant the linear feature is. Then, the process between point A and point B can represent the whole transition process as shown in figure 3c. It is noted that the transition process is symmetrical about the middle point approximately. Thus, we assume that point A and point B are symmetrical about the middle point, and the sum of α and β is 1. The change of parameter χ is only related to parameter α (or parameter β), as shown in the diagonals in figure 3b (also in figure 3a). Parameter χ changes little when parameter α is about 0.2 or larger. In figure 3c, three different situations are carried out to study the influence of parameter α on parameter χ. In each situation, points (A and B) are set to be different positions, and their parameters were calculated respectively in table 1. The parameters α are set as 0.20, 0.25, 0.15 respectively in three different situations marked with S1, S2 and S3. For S2 and S3, both of the percentages of α changing to S1 are 25%, while the percentages of χ changing are only 5.15% and 6.76% respectively, which means the percentage change of χ is much less than α. In addition, linear trends of these three ideal models are calculated according to the points and by regression method which are marked as h_0 in table 1.

The linear trends are also calculated by the values of point A and point B with Eq(5) which are marked as h in table 1. It is noted that although the positions of points are different, the trend obtained according to the points is almost the same as that obtained by regression method. The error percentages are 2.36%, 2.25%, 1.38% respectively, which means that we don't have to know the exactly positions of point A and B (the values of parameters α and β). We can approximate the value of χ. Thus, in the following sections parameter α is set as 0.2, and parameter χ is 0.2164

2.2 The prediction method of transition process

Eq. (8) shows the quantitative relationship among linear trend, instability parameter, and amplitude of change. There is a linear relationship between linear trend and instability parameter; and there is the quadratic function relationship between linear trend and amplitude of change. We did reveal this quantitative relationship much more than in theory but in real time series (Yan et al, 2016). Based on this relationship, we are going to create a new method to deal with the problem that the transition process has not finished. During the real time sequence, the system transits away from the original state, but it has not reached to a new state as shown in figure 4. The red line represents the period which has been experienced, while the gray line represents the period which has not been experienced. Based on the system states which are far away from the original state, a quasi linear extension of the transition process is established (dash line). Then the parameters v and h are obtained by Eq. (4). Assuming that the parameter k satisfies the statistics in the history of the system, the parameter u can be predicted by Eq. (8), and the end moment is also predicted.

$$\begin{cases} x_t = x_{t-1} + kt(x_t - u)(v - x_t) \\ x'_t = x_t + \eta_t \end{cases} . \tag{9}$$

As shown in figure 5, four ideal time sequences are constructed by using the logistic model and random numbers as Eq. (9), where η_t represents the random number. An entire time sequence with 500 moments is shown in figure 5a and three other lengths of time sequences are shown in figures 5b, 5c and 5d respectively. The

parameters v, u and k of the logistic model are set as -1.0, 2.0, 0.1, for the ideal time sequence, and the random number is limited in 0-1. The parameters v, h are obtained by regression method before making prediction. It has to be noted that in this ideal time sequence there is just one abrupt change, which means that we have no way to obtain the value of the parameter k by counting many changes. Thus parameter k is given directly, and the prediction of the end state (moment) is drawn in figure 5b, 5c and 5d. For the entire time sequence, there are 500 moments as shown in figure 5a. In figure 5b, only 240 moments are given, and the other moments are unknown. Then, we obtain parameters v and h by regression method. The parameter u is calculated with Eq. (8). The blue line represents the prediction result. The transition process would be ended in moment 342 with the end state value 2.92. In figure 5c, the end moment and end state are predicted to be 356 and 2.65 respectively when the time sequence is given 250 moments. In figure 5d, the time sequence is given 260 moments. The end moment and end state are predicted to be 359 and 2.58 respectively. The end moment and the end state of the prediction result match the presetting lines. The results also show that the longer the transition process experience, the more accurate the prediction.

3. Results

In order to test the validity of this prediction method in a real climate system, we apply this method to predict the uncompleted transition process of the PDO. The PDO index data used is from website of the University of Washington (http://research.jisao.washington.edu/pdo/). The time period from January of 1900 to November of 2015 is studied as the training data, and the time period from December of 2015 to April of 2017 is used as the test data. During the following research, a transition process starting from 2011 is studied. According to the prediction method, several parameters have to be determined in advance. We first determine parameter k .

3.1 Threshold of parameter *k*

Parameter *k* characterizes the stability of the system during climate change, which means that we can get the value of parameter *k* by counting all abrupt changes of the PDO index. The histogram in Figure 6a shows the PDO time sequence from January of 1900 to November of 2015, and it shows that the PDO went through several changes. The green dots in Figure 6a are parameter *k* when the sub-sequence length takes 20 years. In the early 1940s and late 1970s, there are two main transitions of the PDO. The absolute value of the parameter *k* is large, which means that the system is much more unstable during this two transition processes. In the 1940s, the PDO transits from a positive phase to a negative phase, and $k < 0$, whereas the situation in the 1970s is the opposite. Figure 6b shows more *k* values corresponding to the different sub-sequence lengths (as indicated by X-axis, the variation range of the sub-sequence is 20-60 years, with an interval of 1 year). The Y-axis is the start moment, and the locations of the dots indicate the start moments for the corresponding sub-sequence lengths. In particular, the blue dots represent that parameter *k* is negative, and the red dots represent that it is positive. There are more dots in the left side region than in the right side region in figure 6. This is because when the length of sub-sequence is short, the amplitude is also often small. More transition processes are detected. When the length of the sub-sequence reaches or exceeds 50 years, the transition change mainly begin in the 1940s and 1970s, which are also investigated in other research (Shi et al, 2014). The transition processes in these two periods correspond to large *k* values, which means that these two transition processes are more unstable than others. More statistical results indicate that the threshold distribution of parameter *k* values in historical transition processes exhibit multiple peaks (Figure 7). Specifically, the highest peak with the largest probability is located near to 0. The *k* value is small, which indicates that the abrupt changes are stable. There are some peaks on the left side and right side of zero. When $k<0$, the PDO time sequence transits from the positive phase to the negative phase, which the threshold of the *k* peak is wide and the probability is small; when $k>0$, the PDO time

sequence transits from the negative phase to the positive phase, which the threshold of the k value is narrow and the probability is large. This indicates that the two transitions, which one of them is that the system changes from the positive phase to the negative phase, and the other is that the system changes from the negative phase to the positive phase, are not symmetric, and the latter is more stable. Because there is a difference in parameter k when the selected sub-sequence length is different, Figure 7 also shows the statistical properties of parameter k when the sub-sequence length is 20, 30, 40, 50, or 60 years. When the length of the sub-sequence is 20 years and 30 years, there is only one main peak in the distribution of k values, and the parameter k value of the peak is about 0, which means that the transition change is more stable than the other situations. When the length of the sub-sequence is 40, 50, or 60 years, there are two main peaks. The peak value on the side of $k>0$ is not considerably different, which indicates that the stability degree of the transition change from negative to positive is consistent; the location of the peak value on the side of $k<0$ moves to the left as the sub-sequence length increases, which means that the sub-sequence is longer, the amplitude of detected transition change is larger, and it is more unstable. From the perspective of the value, a k value in the range of (-10, 10) accounts for 80.2% of all k values, a k value in the range of (-5, 5) accounts for 74.2%, and a k value in the range of (-2, 2) accounts for 58.6%. In the following studies, the k value is mainly set in the range of (-2, 2).

3.2 Values of the initial state *v* and linear trend *h*

We use the method proposed in section 2.2 to analyze the transition changes of the PDO. With different lengths of sub-sequences, three climate changes are detected to start from 1976, 2007 and 2011 respectively. In figure 8, the transition changes starting from 2007 and 2011 are shown, while the transition process starting from 1976 has not been shown. In table 2, parameters v and h are obtained by regression method for the transition processes starting from 2007 and 2011. When the length of sub-sequence is 10 years or 20 years, only the transition process starting from 2011 is

detected as shown in figure 8a and figure 8b. The parameter v is calculated with the sequence before 2011. Then, the linear trend parameter h is calculated with the segment after 2011. For the transition process starting from 2011, the values of initial state were detected to be -0.45 and -0.03 when the length of sub-sequence is 10 years or 20 years respectively, and both the linear trends are 1.054/month. When the lengths of sub-sequences are set as 30 and 40 years, the transition process began in 2007 as shown in figure 8c and figure 8d, and the values of initial state are 0.36 and 0.41, respectively, with an linear trend of 0.227/month. When we detect the transition process in a sub-sequence, the percentile threshold method (Huang, 1990) is used. Then, a transition process in the sub-sequence is detected (Yan et al, 2015, 2016). The change with the largest amplitude will be detected. The start moment of the transition change is identified to be 2011 as shown in table 2.

In figure 8, it is noted that the PDO time sequence is leaving the stable state from the start moment. The transition change occurs over a period of time, which is called the transition process. When the transition process has not finished, it appears to be increasing part. In order to detect whether there are other transition processes, we change the length of the sub-sequences to yearly intervals. That is, the sub-sequence length is set as 10, 11, 12, ⋯, up to 60 years. Then, the initial state v and the linear trend h of these transition processes are obtained as shown in figure 9. When the sub-sequence length is set less than approximately 40 years, the transition processes are detected only twice. One began in 2007, and the other began in 2011. The value of parameter h is unchangeable nearly for each transition process, while the value of parameter v is changing when the length of sub-sequence is different. In particular, the transition process starting from 2007 is detected for the sub-sequences of about 30-40 years, and the value of parameter v is in the range of (0.28, 0.45). The transition process starting from 2011 is detected for the sub-sequences of about 10-30 years, and the value of parameter v increases as the length of the sub-sequence increases, whereas the variation range of parameter v is (-0.48, 0.12), which is significantly different from the situation of the transition process starting from 2007.

3.3 Prediction of the uncompleted transition process beginning in 2011

After the threshold ranges for parameters *k, v,* and *h* are determined, according to the quantitative relationship, we can calculate the end state and the end moment of the transition process. Using the transition process in 2011 as an example, we study the ending state and end moment for the PDO index transition process. According to the research results that are presented in Sections 3.1 and 3.2, the parameter is h=1.054/month in this transition process, and the threshold range of parameter k is determined to be (0, 2). The range of parameter v is determined to be (-0.48, 0.12), and the variation situation of parameter u and end moment with parameters k and v are shown in Figure 10. The results indicate that the threshold range of parameter u for the ending state is (1, 7), and the time range of the ending moment is (2013, 2017). According to the probability of parameter k, the end moment of this transition process is about 2015, and after that time, the sequence stops to increase, approaching to a stable state with value of 1.6.

In figure 11, a sketch map is displayed to briefly explain how the prediction method works. The PDO time sequence is displayed as a black line. The period during 2006~2011 is detected as the initial state, and a transition process is increasing from this initial state. It is not able to be known whether the increasing process has been completed or not. Based on the linear regression method, the initial state and the linear trend are obtained and shown as purple dash lines. Then by the method proposed in section 2.2, all possible end states of this transition process are obtained with Eq. (8) as shown in figure 10, and the most likely end state is marked as a green dash line.. Unlike the uncompleted transition process of ideal experiment, the transition process has completed in about 2015 since we detected the PDO change in 2016. This transition process started from 2011 and ends in 2015. The initial moment and the end moment are marked as black dash lines. However, we are still not sure whether the PDO finish this transition process completely or not for it it appears at the

end of the sequence. Many statistical methods are not accurate for the detecting both ends of the sequence. Thus, the real PDO sequence during 2016~2017 is added to the end of the PDO time sequence. The PDO value from 2015 to 2017 is almost unchanged, which is consistent with the predicted result.

4. Conclusion and discussion

A novel method had been proposed to identify the transition process of climate change in our previous research. By defining initial state parameter v, linear trend parameter h, end state parameter u, and instability parameter k, a quantitative relationship among these parameters was revealed. Based on the relationship, we develop a method to study uncompleted transition processes. The method is applied to predict ideal time sequences and the PDO time sequence. In the ideal experiments, three different time sequences with different length are constructed. Based on the initial state and the linear trend which the system had experienced, and the given parameter, the end state and end moment of the transition process are predicted. The prediction result does match the ideal time sequence well. For the PDO time sequence, a transition change beginning in 2011 was taken to test the prediction method. The end moment of this transition process is predicted to be 2015. which is consistent with the real time sequence.

In this prediction method, the quantitative relationship among the parameters characterizing the transition process is vital. According to the segment of the transition process which has been occurred, we determine the parameters and predict the end moment and the end state. In fact, this is also a extrapolation method. It is noted that the uncompleted climate change we studied is closed to the end of the sequence. Due to the lack of enough data, it is difficult to study the end of time sequence by using other statistical methods.

Acknowledgements

We thank two anonymous reviewers for their valuable suggestions. This study

was jointly sponsored by National Key Research and Development Program of China (Grant No. 2018YFE0109600), National Natural Science Foundation of China (Grant Nos. 41675092, 41775078, 41875096), Northwest Regional Numerical Forecasting Innovation Team (GSQXCXTD-2020-02), Meteorological scientific research project of Gansu Meteorological Bureau (MS201914).

References

Alexander R, Reinhard C, Andrey G. Multistability and critical thresholds of the Greenland ice sheet. Nature Climate Change 2012; 429-432

Amaya D, Siler N, Xie S, Miller A. The interplay of internal and forced modes of Hadley Cell expansion: lessons from the global warming hiatus. Climate Dyn 2018; 51, 305–319, doi:10.1007/s00382-017-3921-5

Barnett TP, Pierce DW, Latif M. et al. Interdecadal interactions between the tropics and midlatitudes in the Pacific basin. Geophys. Res. Lett.,1999, 26: 615-618.

Cabezas H, Fath BD. Towards a theory of sustainable systems. Fluid Phase Equilibria 2002; 194–197 3, doi:10.1016/S0378-3812 (01)00677-X

Charney JG, DeVore JG. Multiple flow equilibria in the atmosphere and blocking, J. Atmos. Sci 1979; 36, 1205–1216, doi: 10.1175/1520-0469 (1979)0362.0.CO;2

Goldblatt C, Lenton TM, Watson AJ. Bistability of atmospheric oxygen and the Great Oxidation. Nature 2006; 443:683-686, doi: 10.1038/nature05169

Goossens C, Berger A. Annual and Seasonal Climatic Variations over the Northern Hemisphere and Europe during the Last Century. Annals of Geophysics 1986; 4: 385, doi: 10.1016/0040-1951 (86)90317-3

Huang JY. Meteorological Statistical Analysis and Prediction, Beijing: China Meteorological Press 1990; 28–30

Kosaka Y, Xie SP. Recent global-warming hiatus tied to equatorial Pacific surface cooling. Nature 2013; 501: 403–407, doi: 10.1038/nature12534

Li JP, Chou JF, Shi JE. Complete detection and types of abrupt climatic change. Journal of Beijing Meteorological college 1996; 1:7-12

Liu TZ, Rong PPg, Liu SD, Zheng ZG, Liu SK. Wavelet analysis of climate jump. Acta Geophysica Sinica 1995; 38 (2):158-162

Lorenz EN. Deterministic nonperiodoc flow. J. Atmos. Sci 1963; 20:130, doi: 10.1175/1520-0469 (1963)020<0130:DNF>2.0.CO;2

Lorenz EN. Nondeterministic theories of climatic change. Quaternary Research 1976; 6 (4):495-506, doi: 10.1016/0033-5894 (76)90022-3

Lu CH, Guan ZY, Li YH, Bai YY. Interdecadal linkages between Pacific decadal oscillation and interhemispheric oscillation and their possible connections with East Asian Monsoon. Chinese J. Geophys 2013; 56 (4):1084-1094,

doi: 10.1002/cjg2.20012

Mantua NJ, Hare S, Zhang Y, John W, Robert F. A Pacific Interdecadal Climate Oscillation with Impacts on Salmon Production PDO. Bull.amer.meteor.soc 1997; 78 (6):1069-1079, doi; 10.1175/1520-0477 (1997)078<1069:APICOW>2.0.CO;2

May RM. Simple mathematical models with very complicated dynamics. Nature 1976, 261:459–467, doi: 10.1201/9780203734636-5

Mudelsee M. Ramp function regression: a tool for quantifying climate Transitions, Comput. Geosci 2000, 26:293–307, 10.1016/s0098-3004 (99)00141-7

Nozaki K. Abrupt change in primary productivity in a littoral zone of Lake Biwa with the development of a filamentous green-algal community[J]. Freshwater Biology, 2001, 46(5):587-602.

Newman M, Alexander MA, Ault TR, Cobb KM. The Pacific Decadal Oscillation, Revisited. J. Climate 2016; 29: 4399–4427, doi: 10.1175/JCLI-D-15-0508.1

Osterkamp S, Kraft D, Schirmer M. Climate change and the ecology of the Weser estuary region: Assessing the impact of an abrupt change in climate[J]. Climate Research, 2001, 18(1):97-104.

Overpeck JT, Cole JE. Abrupt change in earth's climate system. Annu. Rev. Environ. Resour 2006; 31:1-31 doi: 10.1146/annurev.energy.30.050504.144308

Sherman DG, Hart RG, Easton JD. Abrupt change in head position and cerebral infarction. Stroke 1981; 12 (1):2, doi: 10.1161/01.STR.12.1.2

Shi WJ, Tao FL, Liu JY, Xu XL, Kuang WH, Dong JW, Shi XL. Has climate change driven spatio-temporal changes of cropland in northern China since the 1970s? Climatic Change 2014; 124:163-177, doi: 10.1007/s10584-014-1088-1

Thom R. Stability Structural and Morphogenesis. Sichuan:Sichuan Education Press, 1972

Trenberth KE, Hurrell JW. Decadal atmosphere-ocean variations in the Pacific. Clim. Dyn 1994; 9:303-319, doi: 10.1007/BF00204745

Wei FY. Modern Climatic Statistical Diagnosis and Forecasting Technology, eijing: China Meteorological Press, 1999

Yan PC, Feng GL, Hou W, Wu H Statistical characteristics on decadal abrupt change process of time sequence in 500 hPa temperature field. Chinese Journal of Atmospheric Sciences 2014; 38 (5): 861−873

Yan PC, Feng GL, Hou W. A novel method for analyzing the process of abrupt climate change. Nonlinear Processes in Geophysics 2015; 22:249-258, doi: 10.5194/npg-22-249-2015

Yan PC, Hou W, Feng GL Transition process of abrupt climate change based on global sea surface temperature over the past century, Nonlinear Processes in Geophysics 2016; 23:115–126, doi:10.5194/npg-23-115-2016

Yang XQ, Zhu YM, Xie Q, Ren XJ. Advances in studies of Pacific Decadal Oscillation. Chinese Journal of Atmospheric Sciences 2004; 28 (6):979-992

Yang P, Xiao ZN, Yang J, et al. Characteristics of clustering extreme drought events in China during 1961–2010. Acta Meteorologica Sinica, 2013a, 27(2):186-198.

Yang P, Ren GY. Liu W. Spatial and temporal characteristics of Beijing urban heat island intensity. Journal of applied meteorology and climatology, 2013b, 52(8):1803-1816.

Yang P, Ren GY. Yan PC. Evidence for a strong association of short-duration intense rainfall with urbanization in the Beijing urban area. Journal of Climate, 2017, 30(15):5851-5870.

Zhang YJ, Wallace M, Battisti DS. ENSO-like interdecadal variability :1900-93. J .Climate 1997; 10:1004-1020, doi: 10.1175/1520-0442 (1997)010<1004:ELIV>2.0.CO;2

Table1. The parameters of ideal models

Situations	α	χ	*h0*	*h*	$\lvert h0-h\rvert/h$
S1	0.20	21.64E-2	12.99E-4	12.69E-4	2.36%
S2	0.25	22.76E-2	9.10E-4	8.90E-4	2.25%
S3	0.15	20.18E-2	32.27E-4	32.72E-4	1.38%

Table2. Parameters *v* and *h* obtained with different sub-sequences

Length of sub-sequence	Start moment (year.month)	*v*	*h* ($month^{-1}$)
10a	2011.06	-0.45	1.054
20a	2011.06	-0.03	1.054
30a	2007.11	0.36	0.227
40a	2007.11	0.41	0.227

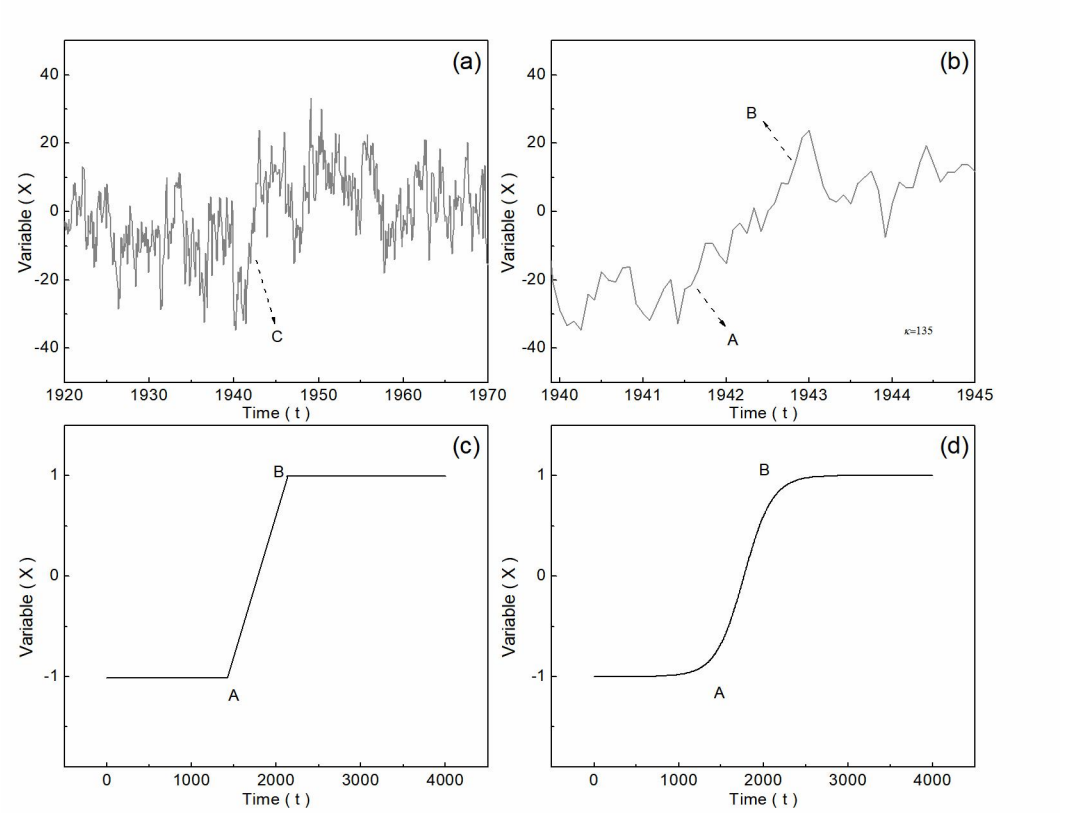

Figure 1. Transition process of abrupt change in real time sequence and ideal time sequence. (a) The PDO time sequence during 1920 to 1970; (b) The PDO time sequence during 1940 to 1945; (c) The transition process presented by piece-wise function; (d) The transition process presented by continuous function

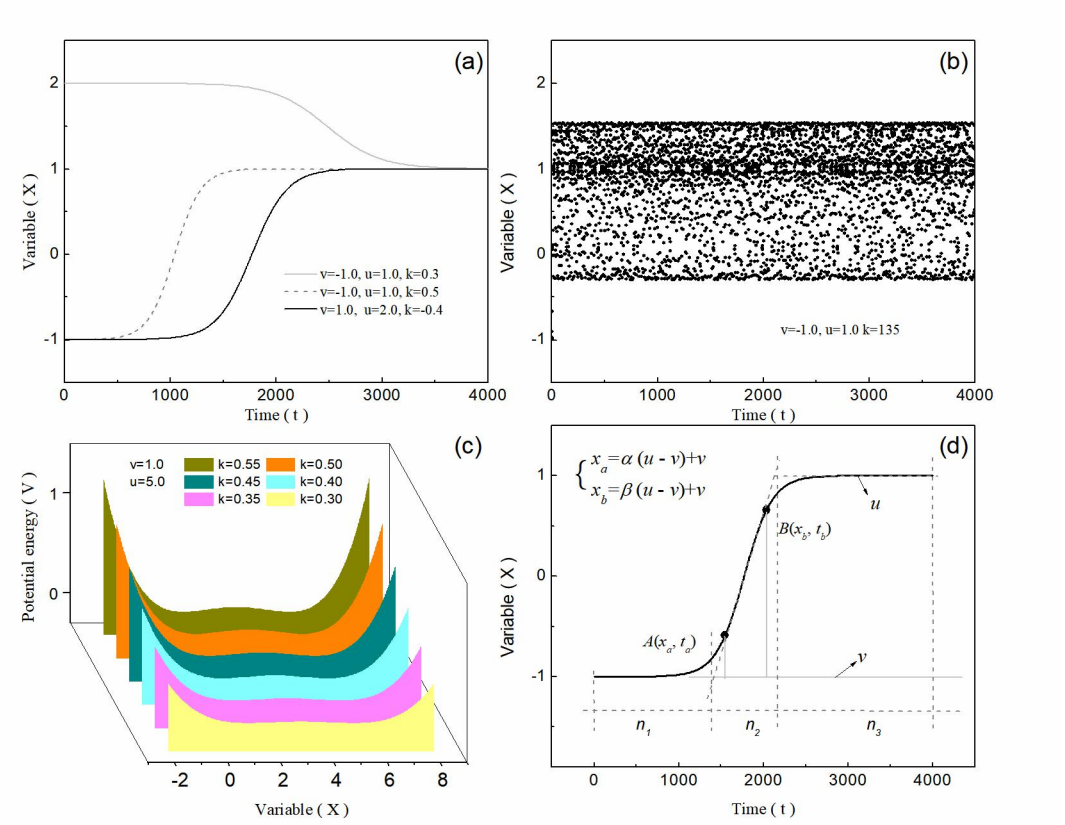

1

2 Figure 2. The system presented by Eq. (2). (a)The transition processes of system
3 swinging between different stable states since the parameters are different; (b)The
4 system stays in unstable states; (c)The generalized potential energy function of system
5 performs differently since the parameters are different; (d)Different segments of the
6 transition process in the ideal time sequence and the system states *x* expressed with
7 location parameters.

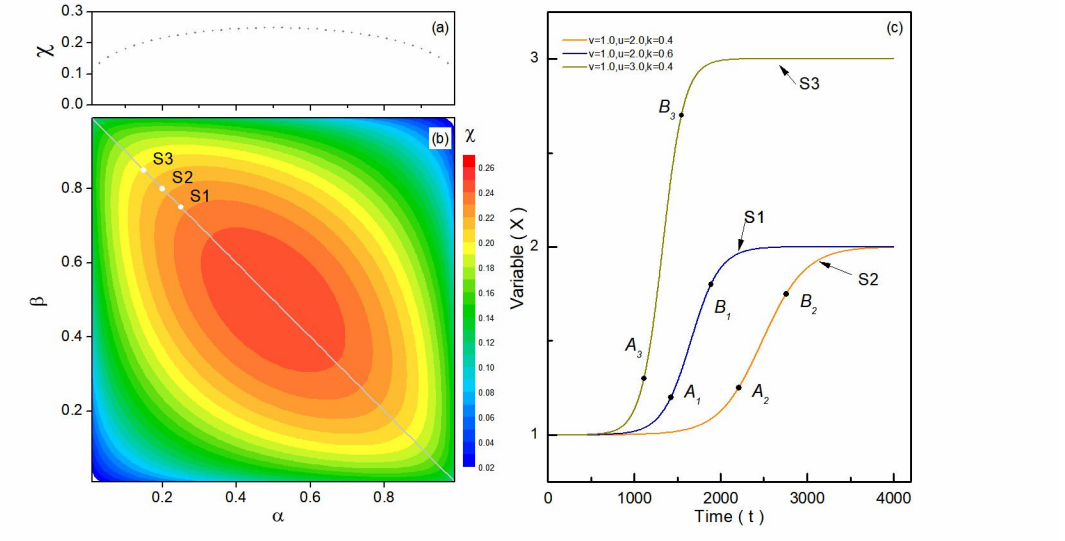

8

Figure 3. The influence of different value of parameters α and β on parameter χ and parameter h. (a) Diagonal section of parameter χ in figure b (gray line); (b) Parameter χ with location parameters α and β; (c)Points A and B stay in different positions in three situations marked as S1, S2, S3.

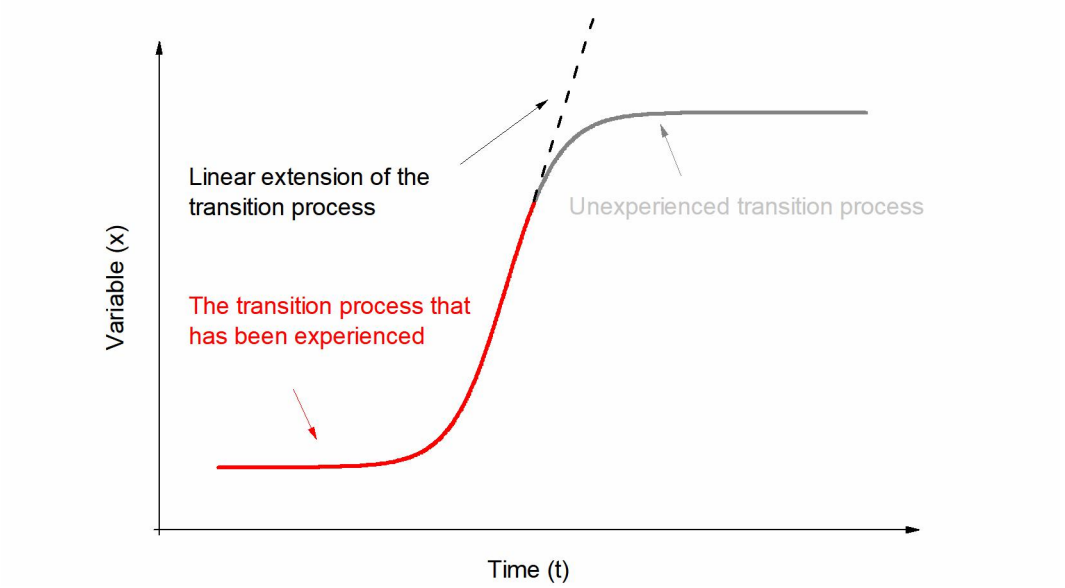

Figure 4. The schematic diagram of prediction method.

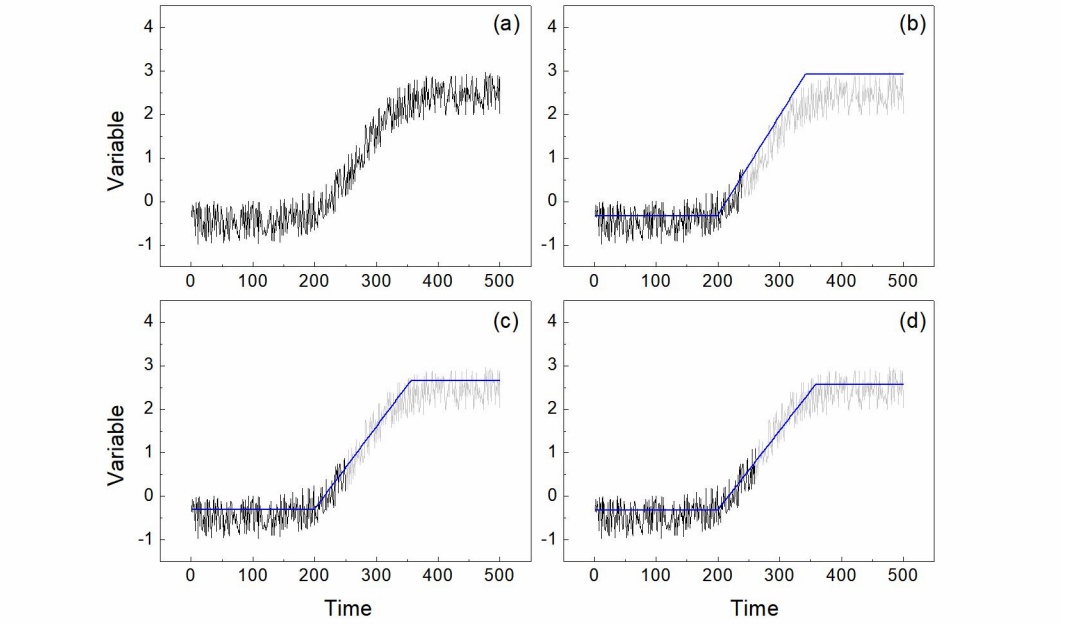

Figure5. The ideal time sequence constructed by the logistic model and random numbers. (a) Completed transition process with 500 moments, Uncompleted transition processes (the gray lines) and their prediction result (the blue lines) with (b) 240

moments, (c) 250 moments, and (d) 260 moments, the light gray lines are the original entire ideal time sequences.

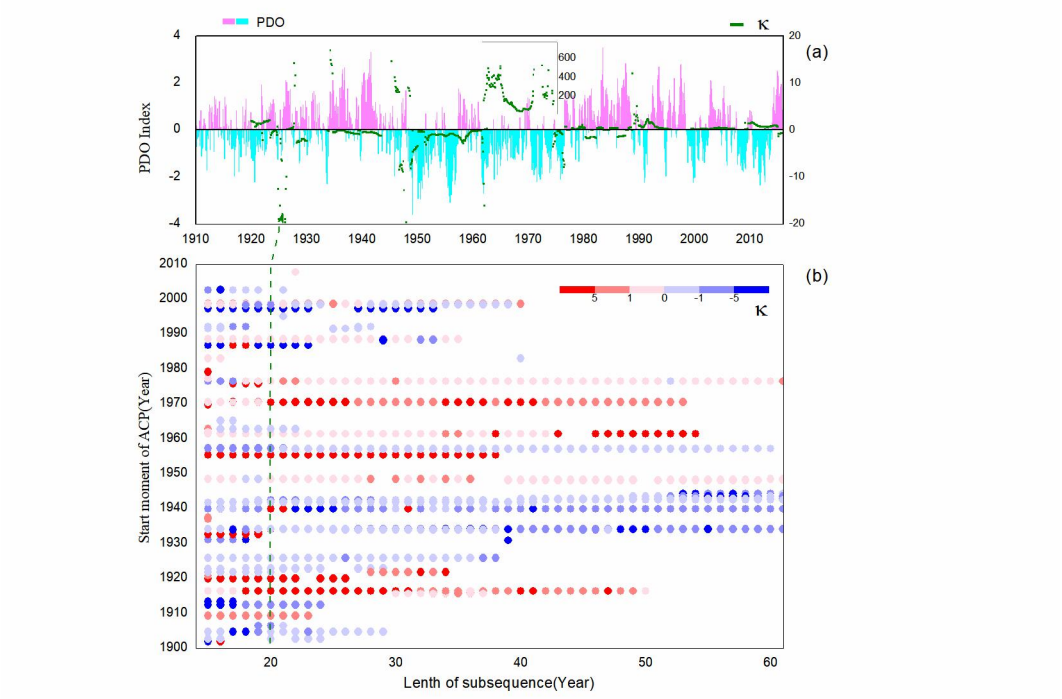

Figure 6. Identification of the PDO time sequence and instability parameter k with different sub-sequence lengths. (a) The X-axis is the year, the histogram in the figure shows the PDO time sequence (left Y-axis), and the green dots indicate the value of parameter k when the sub-sequence is 20 years (right Y-axis); (b) the start moments of transition processes with different sub-sequence lengths (the red color dots represent increasing processes, and blue color dots represent decreasing changes, with deeper colors representing higher values). The X-axis is the sub-sequence length (month), and the Y-axis is the start moment of abrupt change (year).

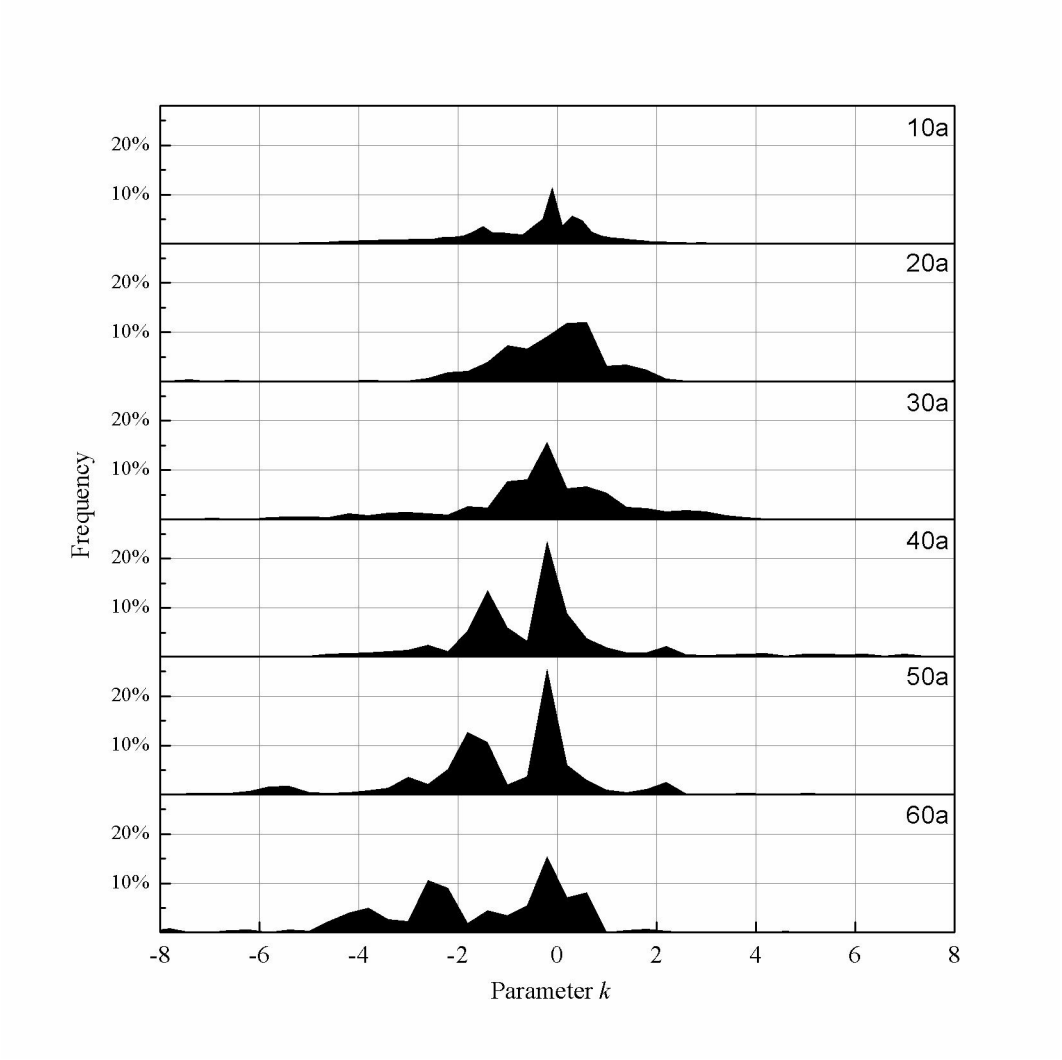

Figure 7. Statistical results of instability parameters for different sub-sequences lengths. The X-axis is the value of the parameter, and the Y-axis is the statistical frequency with a sub-sequence length of 10 years. The gray region in the upper-right corner is for the sub-sequence of 20-60 years.

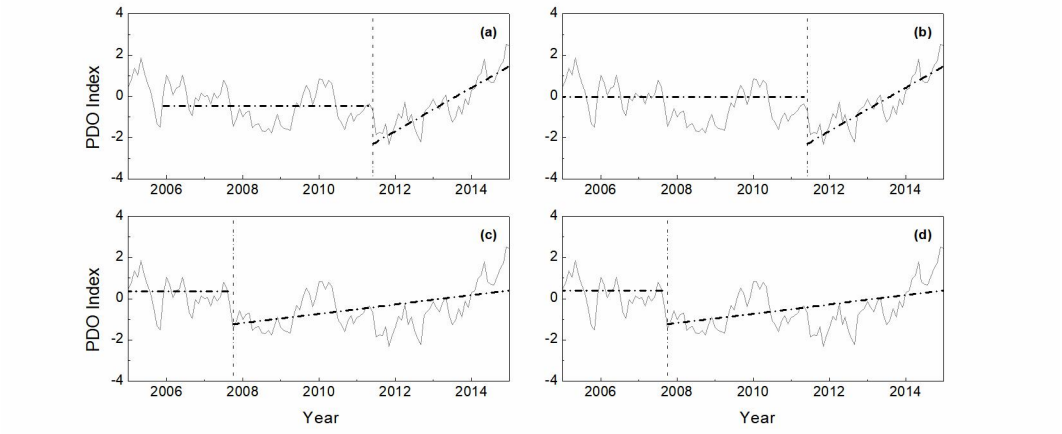

Figure 8. The PDO time sequences and the detection of parameters *v* and *h* when the

sub-sequence was set as (a)10 years, (b)20 years, (c)30 years, (d)40 years. The gray lines represent the PDO time sequence. The horizontal dash lines represent initial states, the slope dash lines represent linear trend lines of the transition process, and vertical dotted lines represent the start moment.

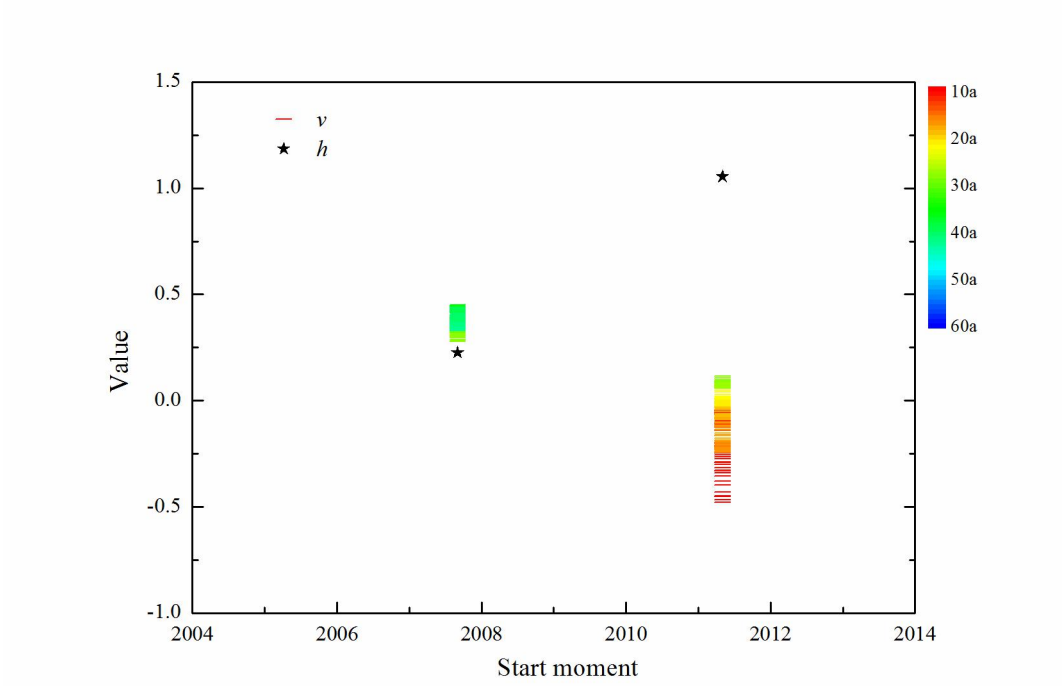

Figure 9. The values of the parameters v and k of two transition processes with different lengths of sub-sequence. The black stars represent the values of parameter h, and the colourful short bar represent the values of parameter v. The colour bar represents years of the sub-sequence length from 10 to 60 in intervals of 1.

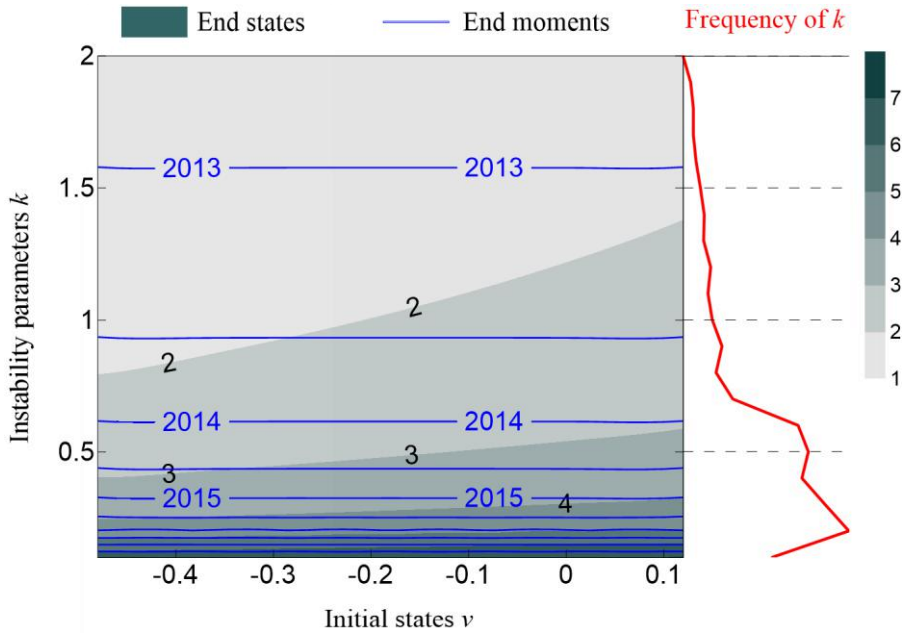

Figure 10. Variation end state and end moment with the initial state parameter v (horizontal ordinate) and instability parameter k (vertical coordinate). The red line on the right side shows the probability distribution of instability parameter k.

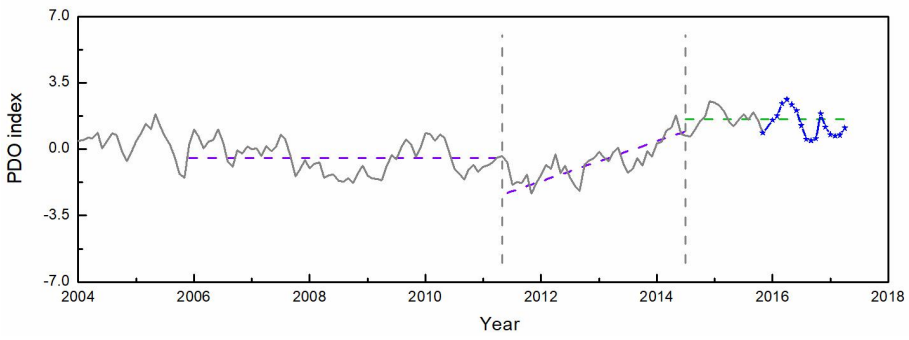

Figure 11. Prediction of the PDO index. The gray line represents the PDO index before 2015; the blue line represents the PDO index after 2015; the gray dash line represent the start moment and end moment; the purple dash lines represent the initial state and the linear trend line, the green line represent the prediction end state.